Mixed-Valence State of Europium in the Misfit Layer Compound $(EuS)_{1.173}NbS_2$

Laurent Cario,* Pierre Palvadeau, Alain Lafond, Catherine Deudon, Yves Moëlo, Benoît Corraze, and Alain Meerschaut

Institut des Matériaux Jean Rouxel, UMR 6502 CNRS, Université de Nantes, Laboratoire de Chimie des Solides − Laboratoire de Physique Cristalline, 2, rue de la Houssinière, BP 32229, 44322 Nantes Cedex 03, France

Received September 10, 2002. Revised Manuscript Received December 10, 2002

A new misfit layer compound $(EuS)_{1.173}NbS_2$ was synthesized, and its structure was solved in a (3+1)*D* superspace using the superspace group $Xm2m(\alpha 00)$ with *X* referring to a pseudo *F* centering. The cell parameters are $a_s = 3.3251(9)$ Å, $b_s = 5.7432(9)$ Å, and $c_s = 22.939(5)$ Å ($V_s = 438.1(3)$ Å^3) with a modulation vector $\mathbf{q} = 0.5867(2)\ \mathbf{a_s}^*$. This compound is built from a regularly alternated stacking of [EuS] slabs (NaCl structure type with two atomic layers) and $[NbS_2]$ slabs (NbS_2 structure type). Mössbauer and XPS spectroscopies as well as magnetic measurements clearly indicate a mixed-valence state for europium with a ratio Eu^{2+}/Eu^{3+} close to 40:60. Bond valence calculations taking into account the modulation of the Eu−S distances ascertain the mixed valence state of europium and indicate that Eu^{2+} and Eu^{3+} ions occupy the same crystallographic site. Moreover, Mössbauer spectra demonstrate that a charge hopping between Eu^{2+} and Eu^{3+} takes place above room temperature. The misfit layer $(EuS)_{1.173}NbS_2$ can be considered as an inhomogeneous mixed-valence compound. Resistivity measurements show that $(EuS)_{1.173}NbS_2$ behaves as a metal and at 3.5 K a strong decrease of the resistivity is observed conjointly with a ferromagnetic transition.

Introduction

During the last twelve years, a systematic study of the structures and properties of the 2D-misfit layer chalcogenides formulated as $[(MX)_m]_{1+x}[TX_2]_n$ was undertaken.[1,2] These compounds have a composite structure which is built from an alternated stacking of [MX] layers of the rock salt type and $[TX_2]$ layers of the CdI_2 or NbS_2 types. Combinations of divalent or trivalent metals M (M = rare earth, Sn, Pb, Sb or Bi) and transition metals T (T = Ti, V, Cr, Nb, or Ta) led to the recognition of numerous new compounds with different alternated stacking sequences as defined by the *m*/*n* ratio. It is now well admitted that the stability of the misfit compounds is attributed to the electron transfer which takes place from the donor [MX] part to the acceptor $[TX_2]$ part.[3] Although such an assumption does not suffer from any doubt when M is trivalent, this explanation seems to be in conflict for divalent metals (M = Sn, Pb). However, accurate chemical analyses have revealed that part of the M^{2+} cations could be substituted by transition elements having higher oxidation states,[4] and it was also proposed that the $[TX_2]$ part could accept part of Sn or Pb lone pair electrons.[5] Both effects restore the donor character of the [MX] layer and this explains the stability of the misfit compounds with divalent metals.

Numerous misfit compounds containing early trivalent rare earths are known. However, one has to recall that binary monochalcogenides LnX (NaCl structure type) contain either Ln^{3+} ions (from La to Sm, and from Gd to Tm) or Ln^{2+} ions with Ln = Sm (only at ambient pressure), Eu, and Yb.[6] Consequently, rare earth misfit compounds with Ln = Sm, Eu, or Yb are of special interest regarding the question of their stability. Would such compounds contain Ln^{2+} or Ln^{3+} ions?, and in the case of Ln^{2+}, would a substitution of the rare earth by the transition element be sufficient to stabilize the structure? Although several samarium misfit compounds are known and contain mostly Sm^{3+} ions, only one misfit compound is reported with europium and ytterbium. The existence of the $(YbS)_{1.23}NbS_2$ compound was mentioned in ref 1, but the oxidation state of Yb in this compound remains unknown. In contrast, for the europium misfit compound $[(EuS)_{1.5}]_{1.15}NbS_2$ the two questions mentioned above, namely the electronic (charge-transfer mechanism) and substitution conditions, were answered.[7] In this last compound the [EuS] slabs are made of three atomic layers and the europium

* To whom correspondence should be addressed via e-mail: laurent.cario@cnrs-imn.fr.

(1) Wiegers, G. A.; Meerschaut, A. *Materials Science Forum*; Meerschaut, A., Ed.: Trans. Tech. Publications: Zurich, Switzerland, 1992, vols. *100 & 101*, p 101.

(2) Rouxel, *J. C. R. Acad. Sci. Paris IIb* **1996**, *323*, 41.

(3) Cario, L.; Moëlo, Y.; Meerschaut, A. *C. R. Acad. Sci. Paris IIc* **1999**, *2*, 617.

(4) Moëlo, Y.; Meerschaut, A.; Rouxel, J.; Auriel, C. *Chem. Mater.* **1995**, *7*, 1759

(5) Wiegers, G. A. *Prog. Solid State Chem.* **1996**, *24*, 1.

(6) Cox, P. A. *The Electronic Structure and Chemistry of Solids*; Oxford Science Publications: New York,1987.

(7) (a) Cario, L.; Lafond, A.; Palvadeau, P.; Deudon, C.; Meerschaut, A. *J. Solid State Chem.* **1999**, *147*, 58. (b) Cario, L.; Meerschaut, A.; Deudon, C.; Rouxel, J. *C. R. Acad. Sci. Paris IIc* **1998**, *1*, 1269.

10.1021/cm020903m CCC: $25.00
Published on Web 01/22/2003

atoms are located in two different crystallographic sites. But more important is that these different europium atoms were found to have distinct oxidation states (2 Eu^{2+} for 1 Eu^{3+}). Consequently, the stability of the compound was ensured by the mixed-valence state of europium authorizing a charge transfer between the slabs. The present paper is dealing with the crystal structure determination and the study of the physical properties of a second europium misfit layer compound, with composition $(EuS)_{1.173}NbS_2$. This compound contains a classical two-atom-thick [EuS] layer with a unique crystallographic site for the europium atoms. To understand the stability of this compound, its crystal structure has been solved using the super-space approach. More, special attention has been paid to characterizing the oxidation state of europium by means of Mössbauer and X-ray photoelectron spectroscopies. Finally, the magnetic properties and the conductivity of this compound have been measured.

Experimental Section

Synthesis. $(EuS)_{1.173}NbS_2$ was prepared from a mixture of EuS (Cerac 99.9%), Nb (Fluka 99.99%), and S (Fluka 99.9%) in the proportion 6:5:10, respectively, with the aim to synthesize the misfit compound $(EuS)_{1.20}NbS_2$. The mixture was sealed in a quartz tube under vacuum ($p \approx 10^{-2}$ atm) and heated with the following temperature profile: the temperature was first raised with a rate of 15 °C/h up to 440 °C for a stage of 2 days, and then up to 900 °C at the same rate for a stage of 7 days. The intermediate reaction product was ground and combined with a small amount of iodine (<3 mg/cm^3) to favor crystallization; it was then reheated at 950 °C for 10 days and air-quenched.

Chemical Analysis. Semiquantitative chemical analyses were performed with the use of a scanning electron microscope JEOL 5800 equipped with a microanalyzer. It revealed that the reaction product was a mixture of several phases. Analysis of large black platelets gave a homogeneous composition (at. %, mean of 4 spot analyses): Eu 20.4(3), Nb 18.3(3), S 61.3(6), which led to the formula $Eu_{1.05}Nb_{0.95}S_{3.17}$, in good agreement with the structural formula of the title compound $Eu_{1.173}Nb_1S_{3.173}$ (at. % Eu 21.9, Nb 18.7, S 59.4). Within the same batch, analyses of small black platelets with a hexagonal shape gave the composition (at. %, mean of 10 spot analyses): Eu 24.1(1), Nb 15.9(1), S 60.0(6), which, on the basis of 22 S atoms, led to the formula $Nb_{8.82}Eu_{5.85}S_{22}$, close to the structural formula of the commensurate composite compound $Nb_8Eu_6S_{22}$ recently described by Khasanova et al.[8]

X-ray Data Collection and Reduction. Numerous crystals of $(EuS)_{1.173}NbS_2$ were tested for quality (intensity and shape of the spots) with a Stoe image plate system (IPDS), and the best crystal was selected for subsequent data collections. To get the best data, two measurements were carried out. First, the intensities were collected on the Stoe IPDS diffractometer. A medium range resolution mode (plate at 80 mm limiting $\sin(\theta)/\lambda$ up to 0.57 Å^{-1}) and a rather long exposure time (720 s) were chosen to increase the number of observed satellites. A second measurement was done on a Nonius CAD-4F diffractometer to collect the intensities of the main Bragg reflections of both subsystems (NbS_2 and EuS) up to higher $\sin(\theta)/\lambda$ (0.75 Å^{-1}).

All reflection sets were consistent with the orthorhombic symmetry and a metric that could be described in a 3D orthorhombic Bravais *P*-centered lattice ($a \approx 16.6$ Å, $b \approx 5.7$ Å, and $c \approx 22.9$ Å). However, the composite character of the structure with two sublattices and satellite reflections was clearly apparent on the diffraction pattern. Satellite reflections with order higher than one were hardly observable and subsequently were not taken into account in the data reduction. The unit cell parameters were refined with the U-FIT program[9] from 40 selected reflections centered on the CAD4 diffractometer and indexed in the (3+1)-*D* space: $a_s = 3.3251(9)$ Å, $b_s = 5.7432(9)$ Å, $c_s = 22.939(5)$ Å, $\mathbf{q} = 0.5867(2)\ \mathbf{a_s}^*$, and $V_s = 438.1(3)$ Å^3.

A detailed description of the theory of the (3+*n*) dimension crystallography can be found in review papers by Janssen et al. and by van Smaalen.[10,11,12] According to this theory, the reflection indices of the [NbS_2] first and [EuS] second subsystems are obtained from (3+1)*D* superspace indexing with the following $\mathbf{W}^1$ and $\mathbf{W}^2$ transformation matrixes, respectively:

$$\mathbf{W}^1 = \begin{pmatrix} 1 & 0 & 0 & 0 \\ 0 & 1 & 0 & 0 \\ 0 & 0 & 1 & 0 \\ 0 & 0 & 0 & 1 \end{pmatrix} \quad \text{and} \quad \mathbf{W}^2 = \begin{pmatrix} 0 & 0 & 0 & 1 \\ 0 & 1 & 0 & 0 \\ 0 & 0 & 1 & 0 \\ 1 & 0 & 0 & 0 \end{pmatrix}$$

Systematic absences were found as $H + K + M = 2n + 1$, $H + L + M = 2n + 1$, and $K + L = 2n + 1$ for the (*H, K, L, M*) reflections. These conditions are in agreement with translation symmetries in the superspace ($^1/_2$, $^1/_2$, 0, $^1/_2$; $^1/_2$, 0, $^1/_2$, $^1/_2$; 0, $^1/_2$, $^1/_2$, 0) which indicates a pseudo-*F*-centered lattice. Special attention was paid to the (0,*K*,*L*,*M*), (0,*K*,0,*M*), and (*H*,*K*,0,*M*) classes of reflection but no other systematic absences were found. The ($m2m$,$\bar{1}\bar{1}1$) (3+1)*D* point group was compatible with the observed diffraction pattern, and we chose the superspace group $G_s = Xm2m(\alpha,0,0)$ with *X* referring to the pseudo *F* centering translation ($^1/_2$, $^1/_2$, 0, $^1/_2$; $^1/_2$, 0, $^1/_2$, $^1/_2$; 0, $^1/_2$, $^1/_2$, 0).

The intensities of the two different data sets collected for $(EuS)_{1.173}NbS_2$ were adjusted for decay (CAD4 set only) and Lorentz-polarization (both sets) and subsequently corrected for absorption via a Gaussian analytical method. Prior to the absorption correction, the crystal shape and dimensions were optimized with the Stoe *X-shape* program on the basis of equivalent reflections.[13] Then the sets were combined after a proper scaling (scale factor IPDS/CAD4 = 7.53) based on 502 main common reflections satisfying $I > 10\ \sigma(I)$. The joined set of 5846 reflections was averaged according to the ($m2m$,$\bar{1}\bar{1}1$) (3+1)*D* point group, and a set of 1002 independent reflections (936 observed reflections with $I \geq 3\sigma(I)$) was obtained. All data treatments, refinement, and Fourier synthesis were carried out with the JANA2000 chain program.[14] Table 1 contains all information about the data collection and reduction.

Structure Determination and Refinement. All refinements were performed on *F* with all reflections included, but reliability factors and electronic residues are hereafter reported for observed reflections only. We noticed that with the choice of the superspace group $G_s = Xm2m$ (α,0,0) the few rejected reflections satisfying the criterion $I > 3\ \sigma(I)$ were of the type (3, *K*, *L*, *M*). In fact, for misfit layer compounds with $\alpha = 0.5867(2)$ close to the commensurate ratio $3/5 = 0.6$, a partial overlap occurs between the (3, *K*, *L*, *M*) and the (*H*, *K*, *L*, 5) reflections. For this reason the (3, *K*, *L*, *M*) reflections were omitted during the refinement (144 rejected reflections with 123 observed one).

The structure of $(EuS)_{1.173}NbS_2$ was first determined by considering the atomic coordinates found by van Smaalen for

(8) Khasanova, N. R.; Van Tandeloo, G.; Lebedev, O. I.; Amelinckx, S.; Grippa, A. Y.; Abakumov, A. M.; Istomin, S. Y.; D'yachenko, O. G.; Antipov, E. V.; *J. Solid State Chem.* **2002**, *164*, 345.

(9) Evain, M. *U-FIT: A Cell Parameter Refinement Program*; I. M. N.-C.N. R. S.: Nantes, France, 1992

(10) Janssen, T.; Janner, A.; Looijenga-Vos, A.; de Wolff, P. M. International Tables for X-ray Crystallography, Vol. C, Mathematical, Physical and Chemical Tables; Wilson, A. J. C., Ed.; Kluwer Academic Publishers: Dordrecht, The Netherlands, 1993; Ch. 9.8.

(11) van Smaalen, S. *Cryst. Rev.* **1995**, *4*, 148.

(12) van Smaalen, S. *Materials Science Forum*; Meerschaut, A., Ed.; Trans. Tech. Publications: Zurich, Switzerland, 1992, vols. *100 & 101*, p 205.

(13) *Stoe: X-Shape, Crystal Optimization for Numerical Absorption Correction*; Stoe & Cie Gmbh: Darmstadt, Germany, 1996.

(14) Petricek, V.; Dusek, M. *JANA2000, a Crystallographic Computing System*; Institute of Physics, Academy of Sciences of the Czech Republic: Praha, Czechoslovakia, 2000.

Table 1. Crystallographic Data, Experimental Details, and Refinement Results for $(EuS)_{1.173}NbS_2$

Crystallographic Data

	[NbS_2]	[EuS]	option (3+1)D
structural formula		$(EuS)_{1.173}NbS_2$	
temperature (K)		293	
color		black	
molar weight ($g \cdot mol^{-1}$)		372.9	
crystal system		orthorhombic	
space group	$Fm2m$	$Fm2m$	$Xm2m(\alpha 00)$
cell parameters:			
a (Å)	3.3293(15)	5.670(5)	3.3251(10)
b (Å)	5.7461(16)	5.744(3)	5.7432(10)
c (Å)	22.926(9)	22.894(14)	22.939(5)
			q = 0.5867 (2) **a***
V (Å^3)	438.6(3)	745.6(9)	438.1(3)
Z			4
calc. density ($g \cdot cm^{-3}$)			5.652
crystal shape		platelet	
crystal size (mm^3)		∼0.135 × 0.110 × 0.020	

Data Collection

	Enraf Nonius CAD-4F	Stoe IPDS
monochromator	oriented graphite (002)	
radiation	MoK-$L_{2,3}$ (λ = 0.71069 Å)	
scan mode	$\omega/2\theta$	
$\sin(\theta)/\lambda$ range	0−0.75	0−0.57

Data Reduction

	option (3+1)-*D*
absorption coefficient (cm^{-1})	205.29
absorption cor. (R_{int} (obs))	Gaussian analytical method (7.1%)
total recorded reflections	5846
independent reflections	958
observed reflections ($I > 3\sigma(I)$)	813

Refinement Results[a]

	option (3+1)-*D*
refinement based on	F ($F(000)$ = 663)
R/R_w obs; R/R_w all (%); n_{obs}/n_{all}	2.87/4.56; 3.50/4.69; 813/958
R/R_w main obs. (%); n_{obs}	2.73/4.29; 758
R/R_w 1st order sat. obs. (%); n_{obs}	10.85/11.97; 55
S	1.06
no. of refinement parameters	31
weighting scheme	$w = 1/(\sigma^2\|F_o\| + (0.0016\|F_o\|)^2)$
residual electronic density $e^-/Å^3$	[−2.43, +2.97]

[a] $R = \Sigma||F_o| - |F_c||/\Sigma|F_o|$. $R_w = [\Sigma w(|F_o| - |F_c|)^2/\Sigma w|F_o|^2]^{1/2}$.

$(LaS)_{1.14}NbS_2$.[15] Using these atomic positions, the refinement of the basic structure converged straight to R = 4.14% for 758 main reflections and 17 variables (Eu and Nb with anisotropic atomic displacement parameters). Observation of the Fourier difference map was essential to introduce the modulation functions. For example, high residual peaks (± 5.6 $e^-/Å^3$) were observed around the Eu atom with a distribution in the superspace that is characteristic of a displacive modulation (see Figure 1a). Refining a displacive modulation function of order 2 for the Eu atom improved the reliability factor (R = 3.25% for all reflections and R = 3.0% for main reflections) and reduced the residual peaks (± 3.3 $e^-/Å^3$; see Figure 1b). In the same way, refining the structure with displacive modulation functions of order one for all other atoms leads to a final reliability factor R = 2.87% for 813 reflections and 31 variables (R = 2.73% for main reflections and R = 10.85% for first-order satellites). At this step the Fourier difference map is featureless with no peaks higher than 2.5 $e^-/Å^3$. Trying to refine the site occupancy factor of the europium atoms does not improve this result. Table 2 presents the fractional coordinates, the anisotropic atomic displacement parameters, and the modulation parameters.

(15) van Smaalen, S. *J. Phys. Condens. Matter* **1991**, *3*, 1247.

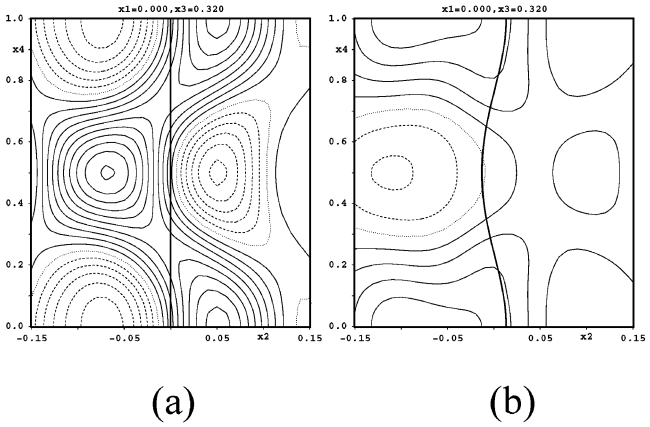

Figure 1. Difference Fourier maps around Eu1 (a) without taking into account the modulated feature of the structure, and (b) taking into account the modulated feature of the structure; contour ±0.5 $e^-/Å^3$.

Table 2. Fractional Atomic Coordinates, Atomic Displacement Parameters, and Displacive Modulation Coefficients for $(EuS)_{1.173}NbS_2$

Fractional Atomic Coordinates

atom	ν	mult.	occ	X	Y	Z	U_{iso}, U_{eq}*
Nb	1	4	1	0	−0.0784(2)	0	0.00688(15)*
S1	1	8	1	0	0.2550(3)	0.06815(6)	0.0083(3)
Eu	2	4	1	0	0	0.32322(2)	0.01319(14)*
S2	2	8	1	0	0.0029(10)	0.19853(10)	0.0161(5)

Atomic Displacement Parameters

atom	U_{11}	U_{22}	U_{33}	U_{12}	U_{13}	U_{23}
Nb	0.0077(3)	0.0053(3)	0.0077(3)	0	0	0
Eu	0.0166(3)	0.0103(2)	0.0127(2)	0	0	0.0003(3)

Displacive Modulation Coefficients

atom (μ)[a]	ν	n	A^{μ}_{n1}	B^{μ}_{n2}	B^{μ}_{n3}
Nb	1	1	0.0040(9)	0.0048(3)	0
S1	1	1	−0.018(3)	0.0030(4)	−0.0013(2)
Eu	2	1	0.0034(6)	0.01238(17)	−0.00085(8)
		2	0.0004(4)	0.0001(5)	0.00042(11)
S2	2	1	−0.0194(15)	0.0057(10)	0.0000(4)

[a] $A^{\mu}_{n2} = A^{\mu}_{n3} = B^{\mu}_{n1} = 0$.

XPS Study. XPS measurements were performed on a KRATOS Axis Ultra spectrometer using the monochromatic Al Kα radiation (1486.6 eV) at 150 W. The instrumental resolution during this work was 0.6 eV corresponding to the full width at half-maximum for Ag $3d_{5/2}$. Because of the low conductivity of the samples along the beam direction (parallel to the stacking direction c), it was necessary to use the charge neutralizer system. All analyses were performed on crystals that were cleaved in air just before being introduced in the spectrometer. Despite these precautions, XPS spectra revealed a contamination of the samples (presence of oxygen). This oxidation effect was more visible for the Eu 3*d* XPS process than for the Eu 4*d* one because of the smaller attenuation length of the 3*d* electrons. Consequently, we have focused our attention on the Eu 4*d* lines.

Mössbauer Study. Mössbauer spectra of $(EuS)_{1.173}NbS_2$ were obtained with a constant-acceleration, automatic-folding Elscint-type spectrometer using a room temperature $^{131}SmF_3$ source in transmission geometry. The Mössbauer sample (collection of crystals ≈100 mg) was studied in the 77−413 K temperature range. At liquid nitrogen temperature an Oxford Instrument variable cryostat was used. Above room temperature, spectra were recorded with a homemade furnace under vacuum. For technical reasons it was not possible to record data at higher temperature. The spectra were computed with a least-squares routine using Lorentzian lines. The isomer

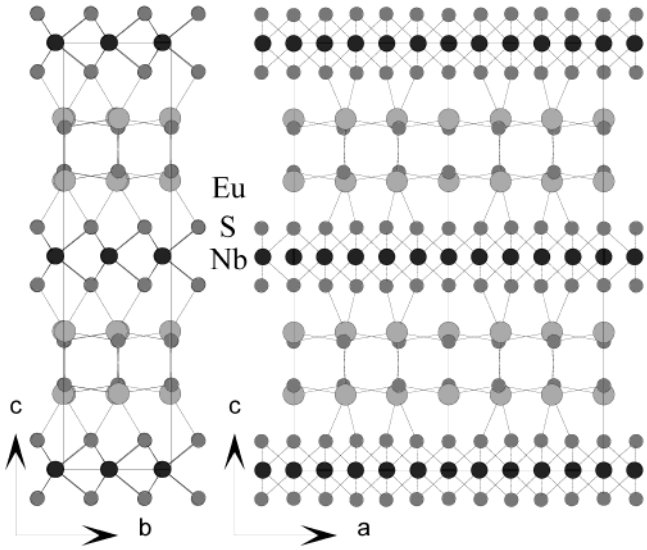

Figure 2. Projection of the structure of $(EuS)_{1.173}NbS_2$ onto the (b, c) and the (a, c) planes. This drawing was done for the commensurate approximation of 5/3.

Table 3. Main Interatomic Distances (Å) in $(EuS)_{1.173}NbS_2$

bond		average	minimum	maximum
Nb	−S1 (×2)	2.472(4)	2.445(6)	2.499(6)
	−S1 (×4)	2.475(5)	2.413(5)	2.537(5)
Eu	−1S2	2.862(6)	2.848(4)	2.890(11)
	−2 S2	2.900(7)	2.866(9)	2.935(9)
	−3 S2	2.932(7)	2.891(9)	2.974(9)
	−4,5 S2 (×2)	2.877(6)	2.780(9)	2.982(8)
	−S1 (×2)		<2.923(9)	
	−S1		<2.868(9)	

shift values were calculated in relation with the resonance line of Eu_2O_3.

Magnetic Study. Both the magnetic susceptibility and the magnetization of $(EuS)_{1.173}NbS_2$ were measured, with the help of a Quantum Design magnetometer, from an assembly of plate-shape crystals (m_{tot} = 7.3 mg) stacked together perpendicularly to the applied magnetic field ($\vec{B}//\vec{c}$). The composition of each crystal was previously checked by EDX analysis. The zero-field-cooled (ZFC) and the field-cooled (FC) magnetic susceptibilities were measured in the 2−300 K temperature range under a magnetic field of 0.10 T. Isothermal measurements were carried out at low temperature (2−8 K) for magnetic fields up to 5.00 T. The data were corrected from the core electrons diamagnetic contribution and from the sample holder contribution. This latter correction was very low (<0.1%) and then was not applied for the low-temperature isothermal data.

Resistivity Measurements. The resistivity of $(EuS)_{1.17}NbS_2$ was measured on crystals in the (*a*,*b*) plane using a conventional four-probes technique with direct current.

Results

Structure Description. Figure 2 shows the projection of the structure of $(EuS)_{1.173}NbS_2$ onto the (*b*,*c*) and (*a*,*c*) planes, respectively. The structure is built from [EuS] and [NbS_2] slabs that are regularly stacked along the *c*-direction. The [EuS] slabs are made of two atomic layers $(100)_{NaCl}$ as in most of the misfit layer compounds $(MX)_{1+x}TX_2$.[1] Eu atoms are coordinated by five S2 atoms belonging to the [EuS] part, and by 1 or 2 S1 atoms from the [NbS_2] part. The [NbS_2] part is similar to the one observed in the binary compound NbS_2, which means that Nb atoms are located in trigonal prisms of S1 atoms. Table 3 summarizes the main interatomic distances (minima, maxima, and averages) obtained for the modulated structure. Because of the mismatch between the [EuS] and [NbS_2] layers, the most modulated interatomic distances are between the Eu atoms (subsystem 2) and the S1 atoms (subsystem 1) as shown in Figure 3. Both the Eu−S distances within the [EuS] slab and between the [EuS] and the [NbS_2] slabs are known for each phase *t* of the superspace (Figure 3). Consequently, the valence of the Eu atoms can be calculated for each phase using the bond valence equation:[16,17]

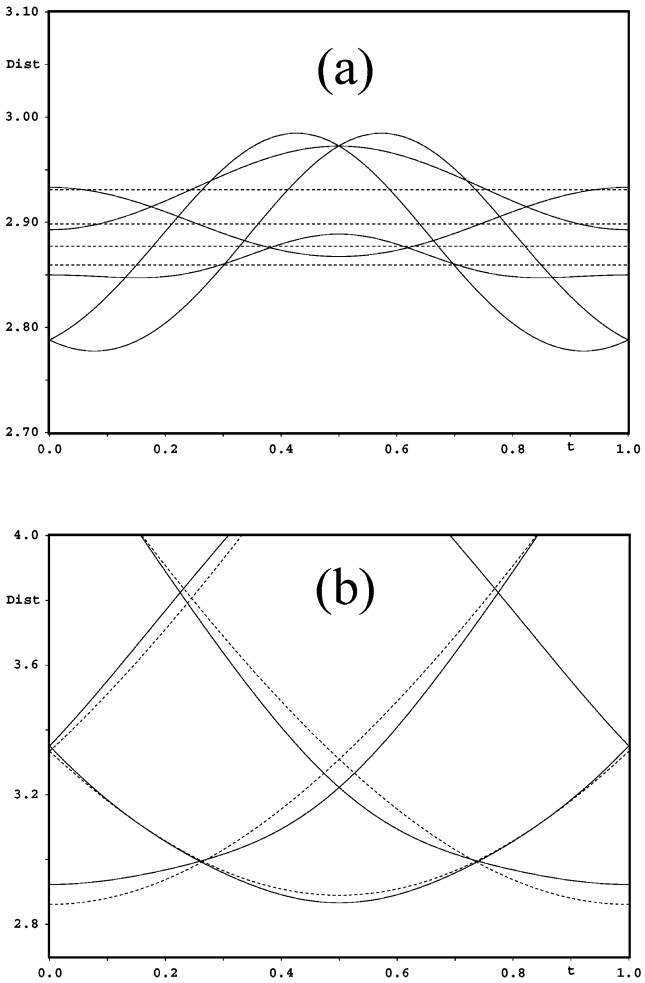

Figure 3. Interactomic distances (a) Eu (subsystem 2) − S2 (subsystem 2), and (b) Eu (subsystem 2) − S1 (subsystem 1), as a function of the phase *t* in the basic structure (dotted line) and in the modulated structure (solid line).

$$V_i = \Sigma \exp [(R°_{ij} - d_{ij})/b]$$

where b = 0.37 is a universal constant, d_{ij} is the interatomic distance (in Å) between atoms i and j, and $R°_{ij}$ is the bond valence parameter depending on the chemical nature of both elements i and j (2.53 for Eu−S distances). Figure 4 shows the variation obtained for the valence of the Eu atoms as a function of *t*. This graph clearly indicates that Eu atoms have an intermediate oxidation state of about 2.55 and which ranges

(16) Brown, I. D. The Bond Valence Method. In *Structure and Bondings in Crystals II*; O'Keeffe and Navrotsky, Ed.; Academic Press: New York, 1981.
(17) O'Keeffe, M. *Struct. Bonding* **1989**, *71*, 161.

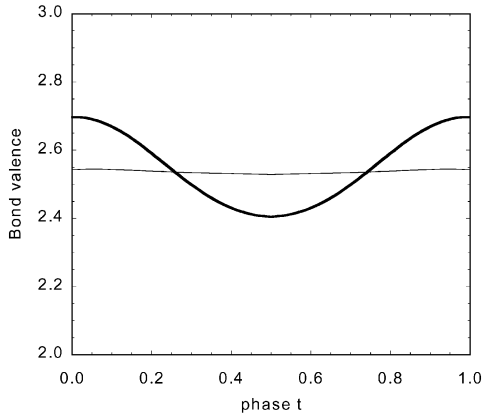

Figure 4. Variation of the periodic function of the calculated valence of Eu versus the phase *t*.

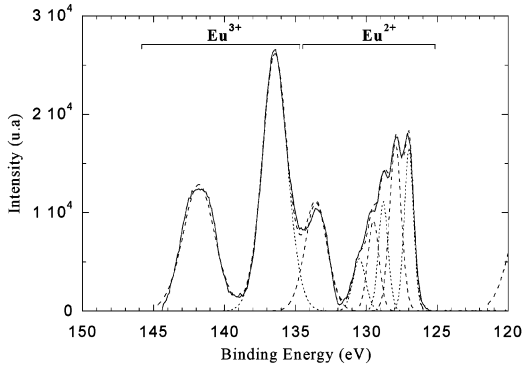

Figure 5. XPS 4d spectra of europium in $(EuS)_{1.173}NbS_2$ (solid line). The dotted lines present the different mixed Gaussian−Lorentzian curves used to fit the experimental spectrum.

from 2.4 to 2.7. Consequently, $(EuS)_{1.173}NbS_2$ appears to be an inhomogeneous mixed-valence compound with both Eu^{2+} (45%) and Eu^{3+} (55%) occupying the same crystallographic site. Such a situation was observed for Eu_3S_4,[18,19] but is completely different from that found for the other europium misfit compound $[(EuS)_{1.5}]_{1.15}NbS_2$, for which Eu^{2+} and Eu^{3+} were located in two different crystallographic sites.[7]

XPS and Mössbauer Spectroscopies. To confirm the presence and the proportion revealed by the structural analysis of both Eu^{2+} and Eu^{3+} species, preliminary XPS studies on $(EuS)_{1.173}NbS_2$ have been undertaken. Such a study was also performed for $[(EuS)_{1.5}]_{1.15}NbS_2$, as in this compound the Eu^{2+}/Eu^{3+} proportion was well-known. For both compounds Eu atoms were found in two different oxidation states, namely 2+ and 3+. As the final Eu state effects are quite complex, the evaluation of the ratio Eu^{2+}/Eu^{3+} was made using the area under the different XPS processes corresponding to Eu^{2+} and Eu^{3+} energy ranges.[20] For both compounds a good approximation of the area of each species was obtained by using a "Shirley" background and by fitting the photolines with 6 and 2 Gaussian−Lorentzian curves for Eu^{2+} and Eu^{3+}, respectively. Figure 5 gives the fitting of the 4d lines obtained for $(EuS)_{1.173}NbS_2$.

Table 4. Evolution of the Isomer Shifts δ of the Lines Corresponding to Eu^{2+} and Eu^{3+} versus Temperature and the Difference $\Delta(\delta)$ between These Two Lines

temp. (K)	δ europium Eu^{2+} [a]	δ europium Eu^{3+} [a]	$\Delta(\delta)$ [a]
77	−12.38	−0.38	12.00
293	−10.66	−0.31	10.35
373	−10.49	−0.37	10.12
393	−10.16	−0.60	9.56
413	−9.79	−1.13	8.63

[a] All values in $mm \cdot s^{-1}$.

The analysis leads to the Eu^{2+}/Eu^{3+} ratio of 45%/55% for $(EuS)_{1.173}NbS_2$ and 65.4%/34.6% for $[(EuS)_{1.5}]_{1.15}NbS_2$, which are in good agreement with the ratios obtained from the structural analysis: 45%/55% and 66.7%/33.3%, respectively.

Figure 6 shows the Mössbauer spectra recorded for $(EuS)_{1.173}NbS_2$ at various temperatures. All spectra are characterized by the presence of two singlets. At 77 K the isomer shift (δ) −12.18 and −0.19 $mm \cdot s^{-1}$ of the singlets are in agreement with the presence of europium atoms at two different oxidation states, Eu^{2+} and Eu^{3+}, respectively. The intensity ratio between both singlets is close to Eu^{2+}/Eu^{3+} = 40:60% and is temperature independent. This situation is similar to that observed in the misfit layer compound $[(EuS)_{1.5}]_{1.15}NbS_2$.[7] However the reason of the presence of the two singlets might be different in these compounds, as Eu^{2+} and Eu^{3+} are located on different crystallographic sites in $[(EuS)_{1.5}]_{1.15}NbS_2$ and on the same site in $(EuS)_{1.173}NbS_2$. Values of the isomer shifts of both singlets δ, as well as of the velocity separation between both singlets $\Delta\delta$ measured for $(EuS)_{1.173}NbS_2$ are reported for all temperatures in Table 4. One can notice that $\Delta\delta$ is strongly temperature dependent, which attests to a charge hopping between Eu^{2+} and Eu^{3+}. In fact, within the temperature range studied, the charge fluctuation frequency between the europium ions is slow compared to the Mössbauer frequency, and two sites with localized electrons are observed. Above 373 K, $\Delta\delta$ decreases linearly, and a simple extrapolation of the curve yields $\Delta\delta = 0$ for a temperature close to 493 K. This means that above 493 K only one singlet corresponding to a mixed valence $Eu^{2.6+}$ is expected. This situation is comparable to what is observed for Eu_3S_4 which is known to be a good example of an inhomogeneous mixed-valence compound.[18,19]

Magnetic Susceptibility Measurements. Figure 7 shows the thermal dependence of the susceptibility and of the inverse susceptibility for 1 mol of europium atoms. There is no difference between the χ_{ZFC} and χ_{FC} curves. The rapid increase of the susceptibility observed as the temperature decreases below 5 K indicates a probable ferromagnetic transition which is far below what is reported for the EuS binary compound (T_c = 16.5 K),[21] and for the 2*D*-misfit derivative $[(EuS)_{1.5}]_{1.15}NbS_2$ (T_c = 8 K).[7] The susceptibility of $(EuS)_{1.173}NbS_2$ follows a Curie−Weiss behavior with a Curie constant of 6.9 10^{-5} $m^3 \cdot K \cdot (mol(Eu))^{-1}$. This value is much smaller than that expected for Eu^{2+} (9.9 10^{-5} $m^3 \cdot K \cdot (mol(Eu))^{-1}$) and indicates that a large part of the europium atoms are in the trivalent state Eu^{3+}. Unfortunately, because of the

(18) Berkooz, O. *J. Phys. Chem. Solids* **1969**, *30* (1), 763.
(19) Massenet, O.; Coey, J. M. D.; Holtzberg, F. *Journal de Physique* **1976**, *37*, 297.
(20) Vercaemst, R.; Poelman, D.; Fiermans, L.; Van Meirhaeghe, R. L.; Laflère, W. H.; Cardon, F. *J. Electron Spectrosc. Relat. Phenom.* **1995**, *74*, 45.
(21) Heller P.; Benedek, G. *Phys. Rev. Lett.* **1965**, *10*, 71.

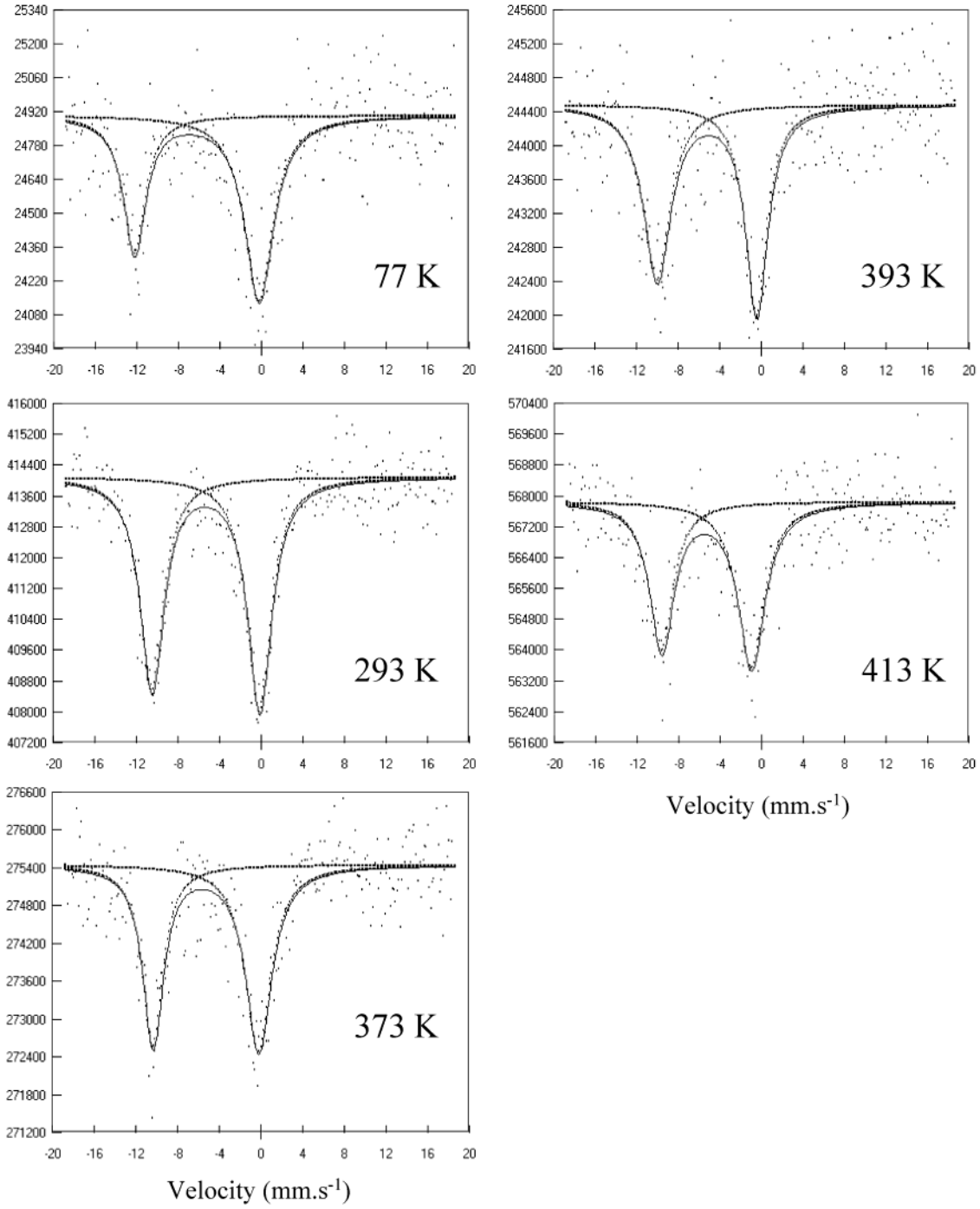

Figure 6. Evolution of the Mössbauer spectra between 77 and 413 K. Two lines are observed that are characteristics of Eu^{2+} and Eu^{3+}. With increasing temperature the split between the two lines is decreasing which attests of a charge hopping. (horizontal scale, velocity in mm·s^{-1}; vertical scale, absorption in arbitrary units).

small amount of available crystals (at 300 K the sample contribution is about 8% of the measured magnetic moment), it was not possible to determine the Eu^{2+}/Eu^{3+} ratio from the high-temperature susceptibility data. However the ratio 40:60 obtained from the Mössbauer study can be used to estimate the Eu^{2+}-only contribution to the susceptibility in the paramagnetic region. Indeed Eu^{3+} is known to be a van Vleck cation, and its contribution can be subtracted from the total susceptibility by using the van Vleck equation limited to the first excited state (lying 500 K above the ground state).[19,22] Figure 7 presents the Eu^{2+} contribution obtained by this way. The slope of $\chi^{-1}(T)$ in the temperature range 20−100 K leads to a Curie constant of $1.3.10^{-4}$ m^3·K· (mol(Eu^{2+}))$^{-1}$ ($\mu_{eff} = 9.1\mu_B$) which is not so far from the expected value C(Eu^{2+}) = $9.9\ 10^{-5}$ m^3·K·(mol(Eu))$^{-1}$ (μ_{eff} = 7.94 μ_B). This calculation confirms that $(EuS)_{1.17}NbS_2$ is a mixed valence compound with a ratio Eu^{2+}/Eu^{3+} close to 40:60.

The low-temperature magnetization versus applied field is shown in Figure 8 for T = 2, 4, 6, and 8 K. In this temperature region the contribution of Eu^{3+} is very low ($J = 0$ in the ground state) compared to that of Eu^{2+}

(22) Van Vleck, J. H. *The Theory of Electric and Magnetic Susceptibilities*; Oxford University Press: London, 1932; p 182.

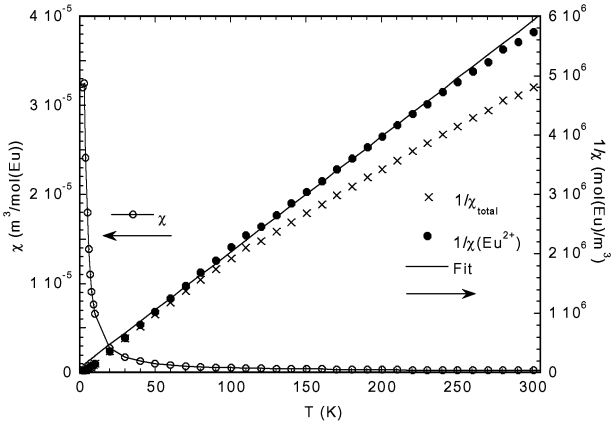

Figure 7. Susceptibility and inverse magnetic susceptibility versus temperature for $(EuS)_{1.173}NbS_2$. The curve with solid circles (●) shows the Eu^{2+}-only contribution per mole of europium atoms obtained after subtracting the calculated contribution of Eu^{3+} ($\chi_{total} = 0.6\chi(Eu^{3+}) + 0.4\chi(Eu^{2+})$). The solid line (−) shows the corresponding curve fit according to the Curie Weiss model: $\chi^{-1} = (T - \theta)/C$ in the 20−250 K temperature range.

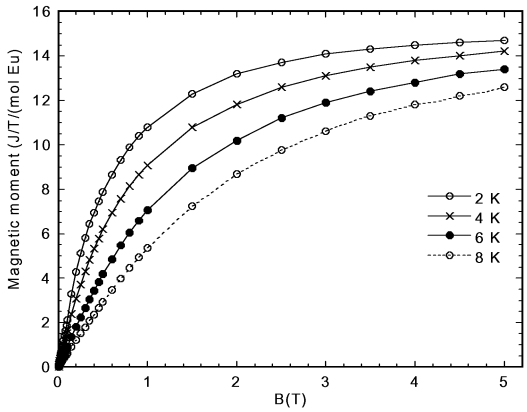

Figure 8. Magnetization curves per mole of europium atoms measured at 2, 4, 6, and 8 K for $(EuS)_{1.173}NbS_2$.

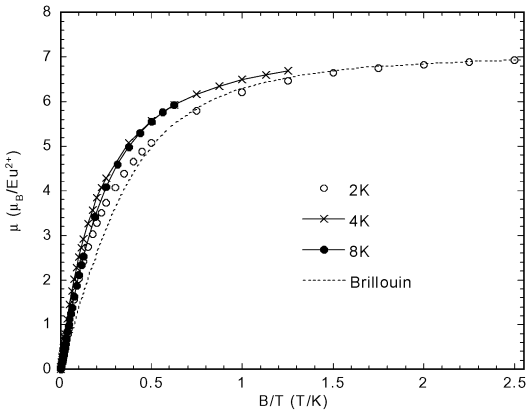

Figure 9. Variation of the magnetic moment per Eu^{2+} ion $\mu(Eu^{2+})$ versus B/T compared to the Brillouin function. The calculation of $\mu(Eu^{2+})$ assumes that the contribution of Eu^{3+} is negligible in this temperature range.

($J = {}^7/_2$). The saturate magnetization of Eu^{2+} should be 39 $J \cdot T^{-1}$ $(mol(Eu^{2+}))^{-1}$. Assuming that the experimental magnetization at 2 K (14.7 $J \cdot T^{-1}$ $(mol(Eu^{2+}))^{-1}$) almost reaches the saturation at 5.00 T, it was possible to roughly estimate a Eu^{2+}/Eu^{3+} ratio of 40:60. Figure 9 shows the B/T dependence of the magnetic moment per Eu^{2+} ion calculated with the previous Eu^{2+}/Eu^{3+} ratio.

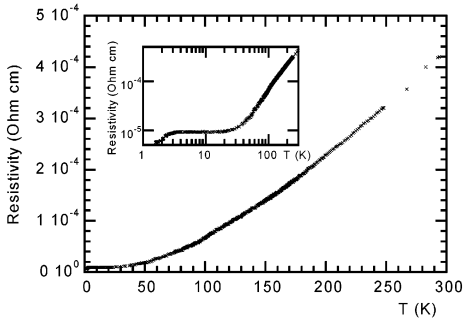

Figure 10. Resistivity versus temperature measured for $(EuS)_{1.173}NbS_2$. The insert shows the breakdown of the resistivity around 3.5 K.

This figure also presents a comparison with the theoretical value deduced from the Brillouin function. The experimental magnetic moment for $T = 2$, 4, and 8 K is slightly higher than the Brillouin's one, especially at low field. This behavior is characteristic of a weak ferromagnetism. This is consistent with a small hysteresis observed on the magnetization loop measured at 2 K ($H_c = 2.4 \times 10^3$ A/m (30 Oe)).

Resistivity Measurements. As shown in Figure 10, $(EuS)_{1.173}NbS_2$ exhibits a metallic-like behavior and its resistivity at room temperature is quite low (about 420 10^{-6} Ohm·cm). At decreasing temperature the resistivity turns aside the classical ρ α T law, and a T^2 temperature dependence is observed which suggests strong interactions between the carriers and the short order magnetic fluctuations. Moreover the log/log plot in the insert clearly shows a breakdown of the resistivity slope versus temperature at 3.5 K. This failure is concomitant with the observed 3D long-range ferromagnetic order.

Discussion

The mixed valence state of europium in the misfit layer $(EuS)_{1.173}NbS_2$ and $[(EuS)_{1.5}]_{1.15}NbS_2$ drives the stability of these compounds. As discussed in detail previously, the stability of the rare earth misfit is related to the charge transfer between the layers.[3] In fact, the reducing character of the [LnS] part (Ln = rare earth), which stabilizes the misfit structure, is ensured only if the $4f^{n+1}$ "level" and the 5*d* bands of the rare earth lie above (or at least sufficiently above) the *nd* bands of the transition metal. In other words, the rare earth has to be found, at least partially, as Ln^{3+} ions ($4f^n$). This condition is easily met for the early rare earth elements, from La to Nd. Compared to the monosulfide LnS, the stability of Ln^{3+} ions is even reinforced in the misfits, on account of the oxidant character of the $[TS_2]$ part. Thus, $(SmS)_{1.25}NbS_2$ is still stable and contains mainly Sm^{3+} ions,[23] while the binary compound SmS contains only Sm^{2+} ions (at ambient pressure). But on going from Sm to Eu, the further decrease in energy of the $4f^{n+1}$ "level" complicates furthermore the charge transfer between the layers. No misfit $(EuS)_{1+x}TS_2$ with T = Ti, V, Cr, Nb, Ta were reported in the literature before the discovery of the two compounds $[(EuS)_{1.5}]_{1.15}NbS_2$ and $(EuS)_{1.173}NbS_2$. This may indicate that in most

(23) Peña, O.; Rabu, P.; Meerschaut, A. *J. Phys.: Condens. Matter* **1991**, *3*, 9929.

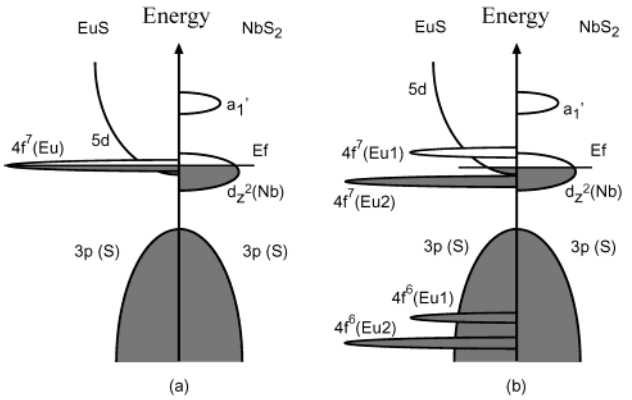

Figure 11. Comparison of the expected schematic band structures of $(EuS)_{1.173}NbS_2$ (a) and $[(EuS)_{1.5}]_{1.15}NbS_2$ (b) showing the position of the $4f^7$ level with regard to the Fermi level in these two misfit compounds.

cases the $4f^{n+1}$ "level" of Eu lies below the highest occupied *d* states of the transition elements, which prevents the charge transfer between the slabs. However, for $[(EuS)_{1.5}]_{1.15}NbS_2$ and $(EuS)_{1.173}NbS_2$, the highest occupied *d* states of niobium and the $4f^{n+1}$ "level" of Eu lie at the same energy, which allows a charge transfer between the [EuS] and $[NbS_2]$ slabs and stabilizes these compounds. In fact, two different situations are encountered in $[(EuS)_{1.5}]_{1.15}NbS_2$ and $(EuS)_{1.173}NbS_2$. For $[(EuS)_{1.5}]_{1.15}NbS_2$ the Eu^{2+} and Eu^{3+} cations are located in two different crystallographic sites and the $4f^{n+1}$ "levels" associated to these cations lie above and below the Fermi level, respectively. On the other hand, for $(EuS)_{1.173}NbS_2$, the Eu^{2+} and Eu^{3+} cations are located in the same crystallographic site and the $4f^{n+1}$ "level" lies just at the Fermi level. On the basis of these differences, a sketch of what could be reasonably expected for the density of states of both compounds is proposed in Figure 11.

In both misfit compounds $(EuS)_{1.173}NbS_2$ and $[(EuS)_{1.5}]_{1.15}NbS_2$ the mixed valence state of europium allows a charge transfer of about 0.6 electron per niobium atoms from the [EuS] to the $[NbS_2]$ slabs which is sufficient to stabilize the structure. It is likely that such a situation (mixed valence and charge transfer) is also prevalent in the recently discovered composite compound $[Nb_7S_{14}][Nb(Eu_3S_4)_2]$ where a $Nb(Eu_3S_4)_2$ layer alternates with a NbS_2 layer, although the authors envisage only a divalent state for Eu.[8]

Conclusion

The structure of the misfit layer compound $(EuS)_{1.173}NbS_2$ has been solved in a (3+1)*D* superspace. This compound is built from a regularly alternated stacking of [EuS] slabs (NaCl structure type with two atomic layers) and $[NbS_2]$ slabs (NbS_2 structure type). Mössbauer and XPS spectroscopy as well as magnetic measurements clearly indicate a mixed-valence state for europium with a ratio Eu^{2+}/Eu^{3+} around 40:60. This mixed valence state allows a charge transfer between the [EuS] slabs and $[NbS_2]$ slabs which stabilizes the structure. Bond valence calculations taking into account the modulation of the Eu−S distances ascertain the mixed valence state of europium and indicate that the Eu^{2+} and Eu^{3+} cations occupy the same crystallographic site. Moreover, Mössbauer spectra clearly show that a charge hopping between Eu^{2+} and Eu^{3+} takes place above room temperature. This behavior is comparable to what is observed at lower temperatures for Eu_3S_4. Similarly to this latter compound, the misfit $(EuS)_{1.173}NbS_2$ can be considered as an inhomogeneous mixed valence compound. This class of compounds has attracted much attention since the discovery of heavy fermion. On behalf of the resistivity measurement we could not discard this possibility for $(EuS)_{1.173}NbS_2$ and further experiments are in progress to answer this question.

Supporting Information Available: Crystallographic information files (PDF). This material is available free of charge via the Internet at http://pubs.acs.org.

CM020903M